1. Yamazawa K, Nakabayashi K, Matsuoka K, Masubara K, Hata K, Horikawa R, Ogata T. Androgenetic/biparental mosaicism in a girl with Beckwith-Wiedemann syndrome-like and upd(14)pat-like phenotypes. J Hum Genet, 2011, 56(1);91-3.
2. Oto Y, Obata K, Matsubara K, Kozu Y, Tsuchiya T, Sakazume S, Yoshino A, Murakami N, Ogata T, Nagai T. Growth Hormone Secretion and its Effect on Height in Pediatric Patients with Different Genotypes of Prader-Willi Syndrome. 2012, Am J Med Genet A. (In press)

２．学会発表

1. 第２５回小児脂質研究会(京都)「Prader Willi 症候群（PWS）の脂肪分布解析と成長ホルモン(GH)療法が分布に及ぼす影響について」阿部美子、田中百合子、村上信行、永井敏郎
2. 第２５回小児脂質研究会(京都)
「肥満 Prader-Willi 症候群(PWS)の脂肪分布の特徴
-アディポサイトカインが高脂血症と糖尿病へ与える影響について-」
田中百合子、阿部美子、村上信行、永井敏郎
3. 第 114 回小児科学会（東京）
「高齢出産は trisomy rescue に起因する母性片親性ダイソミーの発症リスクである：Prader-Willi 症候群 154 例の分子遺伝学的解析」
松原圭子、佐藤智子、鏡雅代、緒方勤、永井敏郎
4. European Human Genetics Conference 2011 (Amsterdam)
"Risk assessment of ART and its related factors in the development of Prader-Willi syndrome"
Matsubara K, Murakami N, Sakazume S, Oto Y, Nagai T, Ogata T.
5. 第 34 回小児遺伝学会（横浜）
「ART および ART 関連因子は PWS の発症リスクとなるか？」
松原圭子、村上信行、坂爪悟、大戸祐二、緒方勤、永井敏郎
6. 61st, The American Society of Human Genetics (Montreal)
"Risk assessment of ART and its related factors in the development of Prader-Willi syndrome" Matsubara K, Murakami N, Sakazume S, Oto Y, Nagai T, Ogata T.
7. 第 45 回小児内分泌学会（大宮）
「ART および ART 関連因子は PWS の発症リスクとなるか？」
松原圭子、村上信行、佐藤智子、鏡雅代、永井敏郎、深見真紀、緒方勤
8. 第 56 回人類遺伝学会（千葉）
「ART および ART 関連因子は PWS の発症リスクとなるか？」
松原圭子、村上信行、佐藤智子、鏡雅代、永井敏郎、深見真紀、緒方勤

Ｈ．知的財産権の出願・登録状況
（予定を含む。）

1．特許取得
なし
2．実用新案登録
なし
3．その他
なし

厚生労働科学研究費補助金（難治性疾患克服研究事業）
研究分担報告書

Prader-Willi 症候群における諸症状の評価と治療効果の判定

研究分担者　村上信行
獨協医科大学越谷病院　准教授

研究要旨

Prader-Willi 症候群（PWS）は、多彩な症状を呈する先天奇形症候群である。我々は、昨年度に引き続き、精神神経症状、側彎症、脂質代謝異常について検討を行った。今年度は、精神神経症状に対して精神科、側彎症に対して整形外科による介入を積極的に行い、専門的見地から PWS に伴う諸症状の評価および治療効果の判定を行った。
精神神経症状については、 1）UPD のほうが欠失よりも IQ が低く、広汎性発達障害特性が高い傾向があり、また母親の QOL も低いこと、 2）PWS の約 20%に何らかの痙攣を合併するものの、難治性痙攣の頻度は低いこと、 3）PWS 患者で認められた左島皮質の低灌流は、食行動の重症度スコアと有意な相関を示すことが明らかとなった。
脂質代謝については、GH 投与の脂肪代謝への有効性、および、心血管系イベント発症のハイリスク群（内臓脂肪が多く、adiponectin が低値）では積極的な介入の必要性が示唆された。側彎症については、PWS 患者では特発性側彎症患者と比較し、腰椎・胸腰椎型側彎が多いことが明らかとなった。
これらの結果から、PWS における治療指針の作成に大きく貢献することが期待される。

共同研究者

田中百合子（獨協医科大学越谷病院　小児科）
竹下絵里（獨協医科大学越谷病院　小児科）
井原裕（獨協医科大学越谷病院　こころの診療科）
尾形広行（獨協医科大学越谷病院　こころの診療科）
中村豊（獨協医科大学越谷病院　整形外科）
小倉加恵子（国立障害者リハビリテーションセンター）

A. 研究目的

Prader-Willi 症候群（PWS）は、多用な症状を呈する先天奇形症候群である。われわれは、昨年度に引き続き、精神神経症状、側彎症、脂質代謝異常について検討を行った。

B. 研究方法

・精神神経症状

1) Prader-Willi 症候群と広汎性発達障害の心理行動症状の比較研究（井原、尾形）

PWS の患者と広汎性発達障害の患者本人に知能検査(WAIS-Ⅲまたは WISC-Ⅲ)、患者と保護者に PARS(Pervasive Developmental Disorders Autism Society Japan Rating Scale)、ADHD-RS-Ⅳ(ADHD-Rating Scale - Ⅳ)、DY-BOCS(The Dimensional Yale-Brown Obsessive-Compulsive Scale)を行う。また保護者に WHOQOL-26(The World Health Organization Quality of Life-26)を行い、PWS 患者のみでは性別、遺伝子型での性格・行動上の比較、また PWS 患者と広汎性発達障害の性格・行動上の問題の比較検討することで、それぞれの特徴を明確にする。

2) 日本人 Prader-Willi 症候群での痙攣の頻度と特徴（竹下）

1998 年以降、獨協医科大学越谷病院小児科で診療した PWS 患者 143 人(性別:男性 83 人、女性 60 人、遺伝子型:欠失 108 人、片親性ダイソミー(UPD)31 人、特殊な染色体異常 4 人)を対象に、診療録と検査結果を後方視的に調査し、痙攣の頻度と特徴を検討した。

3) Prader-Willi 症候群の脳血流の特性（小倉）

PWS 成人 12 名と年齢・性別を一致させた健常成人 13 名を対象とした。PWS 群は食行動評価として全国調査で使用した評価票（Ogura et al., 2008）による介護者インタビューを行い、重症度をスコア化した。画像検査は、脳血流イメージング剤 I123-iodoamphetamine を使用し、triple-detector SPECT system にて、安静閉眼状態で全脳を撮像した。解析は、partial volume effect を補正し、SPM2 により群間比較を行った（有意水準 $p<0.001$, uncorrected)。群間比較で有意な差があった脳領域のうち食行動との関与が推測される領域を関心領域（ROI）として設定し、ROI と食行動の重症度スコアとの相関を検討した。

・脂質代謝異常（田中）

BMI 25 以上の肥満 PWS24 例について、体脂肪分布、アディポサイトカイン、心血管系疾患の risk factor である脂質異常と II 型糖尿病(Tcho, LDL , HDL, TG, HbA1C）の関連について検討した。

・側彎症

PWS 症候群における成長ホルモン療法と側弯症の関

連：急速進行例について（村上）

成長ホルモン療法開始後に9か月間に側彎症が発症・増悪した例に対し、増悪因子を検討した。

PWSにおける側彎症（58例）と特発性側彎症（56例）との比較研究（中村）

PWS群は、遺伝的に確定診断された197例のうち側彎症を認めたのは62例（31.5%）で2年以上経過観察可能であった58例（男34、女24）を対象とした。平均年齢は17.9歳で、GH治療は32例でおこなっていた。一方特発性群は、1年間に継続的に外来で経過観察をおこない、2年以上経過観察可能であった56例（男4、女52）を対象とした。平均年齢は16.9歳であった。これらの症例について1) Lenke 分類 2) Cobb 角（最終経過観察時また手術例では術前）2) L4 tilt 3) Thoracic kyphosis （T2-5およびT5-12） 4) lumbar lordosis （T12-S1） 5) Saggital alignment （C7 plum line）を計測した。また Body Mass index(BMI)と精神発達遅滞の有無についても調査した。

（倫理面への配慮）

本研究の遂行にあたっては、ヒトゲノム・遺伝子解析研究に関す巣倫理指針を遵守し、検体の収集を含めた研究計画については、国立成育医療研究センター、および各検体の収集施設において予め倫理委員会の承認を得ている。検体は、書面によるインフォームドコンセントを取得後に収集している。

C. 研究結果

・精神神経症状

1) Prader-Willi 症候群と広汎性発達障害の心理行動症状の比較研究（井原、尾形）

今年度中ではPWS患者20人（欠失17人、UPD3人）の検査が終了した。検査終了したPWS患者の性別と遺伝子型に分けて WAIS - Ⅲ、PARS、WHOQOL - 26について順に報告する。ただしサンプル数の影響で統計的検定をするまでには至っていない。

性別別では男性が16名（平均23.8歳）、女性が4名（平均25.3歳）で、WAIS - Ⅲの全検査IQは男性が50±8.7、女性が57±11.2、言語性IQは男性が56.3±5.2、女性が62.5±9.5、動作性IQは男性が51.8±11.5、女性が57.8±11.9、言語理解は男性が57±6.1、女性が65.3±14.9、知覚統合は男性が55.7±12.9、女性が63±17.9、作動記憶では男性が55.2±10.6、女性が62.3±14.3、処理速度では男性が53.3±7.5、女性では56±5.5であった。PARSにおいては幼児期ピーク得点が男性では10.4±4.6、女性では9±8.1で、思春期・成人期得点は男性が14.1±5.1、女性が15.3±5.3あった。WHOQOL - 26においてはOQL平均値が男性では3.3±0.39、女性では2.99±0.19であった。

次に遺伝子型に分類すると、欠失型が17名（平均24.3歳）、UPD型が3名（平均23歳）で、WAIS - Ⅲの全検査IQは欠失型が52.3±9.9、UPD型が46.3±1.2、言語性IQは欠失型が58.1±6.9、UPD型が54.3±0.58、動作性IQは欠失型が54.2±12.2、UPD型が46.3±1.5、言語理解は欠失型が59.53±9.1、UPD型が53.7±2.5、知覚統合は欠失型が58.4±14.7、UPD型が50±1.7、作動記憶は欠失型が57.8±11.9、UPD型は50±1.7、処理速度は欠失型が54.5±7.6、UPD型は50±0であった。PARSにおいては幼児期ピーク得点が欠失型では9.8±5.5、UPD型では11.7±3.2で、思春期・成人期得点は欠失型が9.8±5.5、UPD型が20.3±3.1あった。あった。WHOQOL - 26においてはOQL平均値が欠失型では3.28±0.40、UPD型では3.03±0.10であった。

2) 日本人 Prader-Willi 症候群での痙攣の頻度と特徴（竹下）

対象143人中30人（21%）に痙攣の既往があり、欠失24人（全体の80%、欠失の22%）、UPD5人（全体の17%、UPDの16%）、特殊な染色体異常1人（全体の3%）であった。痙攣の特徴は、新生児痙攣2人（7%）、単純型熱性痙攣14人（47%）、複合型熱性痙攣3人（10%）、てんかん8人（27%）、熱性痙攣＋胃腸炎関連痙攣2人（7%）、熱性痙攣＋脱力発作1人（3%）であり、26人（87%）は全般性痙攣であった。発症時期は、1歳以前8人（38%）、1歳13人（43%）、2歳4人（13%）、3歳4人（13%）、4歳1人（3%）であった。脳波を施行した23人中12人（52%）で異常を認めた。

3) Prader-Willi 症候群の脳血流の特性（小倉）

健常対照群と比較してPWS群では、右視床、左島皮質、舌状回~小脳において低灌流、両側前頭葉眼窩皮質、両側角回、左側背外側前頭前野で高灌流が認められた。また、左島皮質の低灌流は食行動の重症度スコアと有意な相関を示した。

・脂質代謝異常（田中）

加齢に伴い、内臓脂肪量(VAT)、皮下脂肪量(SAT)ともに激増したが、GH治療中の18例のVATは年齢に関わらず30cm²以下の低値であった。GH治療が終了した19例は、GH非使用群14例と同様にVAT、SATは高値となっていた。

肥満群は、VAT/SAT（V/S）が低い皮下脂肪有意型肥満が多かった。

肥満群のAdiponectinはVATが少ないと減少し(r=-0.35, p=0.11)、leptin (r=0.67, p<0.001), resistin (r=0.45, p=0.04)はSATと強い正の相関を示した。肥満群のTCho, LDL、TGはadioponectin と負の相関があり(r=-0.59, r= -0.56 , r= -0.56, p<0.05) HbA1CもadiponectinがVAT低い程高い傾向があった（r= -0.42 p=0.08）。 Leptin, resistinとこれらのfactorは相関しなかった。

・側彎症

PWS症候群における成長ホルモン療法と側弯症の関連：急速進行例について（村上）

急速進行例の増悪因子について、身長の伸び、脊椎

の形態異常、脊椎負荷の変化（運動能の変化、体重変化）、傍脊柱筋の増大率や左右差の観点より検討した。その結果、GH 使用による成長率の改善が見られた時期に側彎症が発症・増悪し、また独歩開始による脊椎への加重増加も急性増悪との関連が疑われた。

PWS における側彎症（58 例）と特発性側彎症（56 例）との比較研究（中村）

1) Lenke 分類（PWS 群/ I 群)の内訳は、Type 1(9/26), Type 2(2/5), Type 3 (3/15), Type 4 (0/0), Type 5(32/8), Type 6 (13/2)であった。2) 平均 cobb 角は 32.2° と 35.5°であった（有意差なし)。3) L4 tilt は、10.5° と 9.1°であった(有意差なし)。4) Thoracic kyphosis は、T2-5 で 18.3° と 15.7°(有意差なし)、T5-12 で 17.3° と 10.1°(有意差なし）であった。 5) lumbar lordosis （T12-S1）は、47.2° と 45.5°であった(有意差なし)。6) C7 plum line は、10.5° と 5.3°(有意差なし)であった。また BMI は、26.0 と 19.2 であり(P=0.042、有意差なし)、精神発達遅滞は、100% と 0%（有意差あり）であった。

D. 考察

・精神神経症状

1) Prader-Willi 症候群と広汎性発達障害の心理行動症状の比較研究（井原、尾形）

性別別であるが、知能検査においてはどの IQ においても女性のほうが高かった。PARS（広汎性発達障害評定尺度）においては男女ともに幼児期ピーク得点のカットオフ 9 を越えていて、思春期・成人期得点においてはカットオフ 20 を超えていない。つまり幼児期のほうが広汎性発達障害の特性を有している PWS 患者は多いが、成人になるにつれてその傾向は少しやわらいでいくものと考えられる。ただしともにカットオフは下回っているが得点は高く、家族、特に母親の負担も大きいと思われる。母親の QOL については女性の PWS 患者の母親で低くなっている。

遺伝子型では、どの IQ においても欠失型のほうが UPD よりも高かった。PARS においてはともに幼児期ピーク得点はカットオフを越えていて、さらに UPD においては思春期・成人期得点のカットオフも越えている。つまり欠失型においては幼児期には広汎性発達障害の特性を有しているが、成人になるにつれてその特性は変化していく、しかし UPD 型においては成人になっても広汎性発達障害の特性を有している傾向が高い。そのためか母親の QOL においても UPD 型の母親のほうが低い。

今後はサンプル数を増やし、PWS 患者の特性や PWS 患者と広汎性発達障害の患者特性とを比較し、問題行動に対してどうような対応が適切であるかの指標が得られればと考えている。

2) 日本人 Prader-Willi 症候群での痙攣の頻度と特徴（竹下）

日本の PWS 患者の痙攣合併は 21%であり、過去の海外の報告（26%）とほぼ同様であった。UPD に比し欠失に痙攣合併が多いとの報告もあるが、遺伝子型間で有意な差（p＝0.45）はなかった。57%は熱性痙攣で、てんかんは 27%と少なく、2 歳以下の低年齢の発症が多かった。脳波を施行した患者のうち、52%で異常を認めたが、PWS に特徴的な脳波所見はなかった。PWS の痙攣は、Angelman 症候群と異なり、難治に経過する例は少なかった。

3) Prader-Willi 症候群の脳血流の特性（小倉）

PWS 群の安静時脳局所血流パターンは健常者群とは異なっていた。島皮質の血流低下は、PWS の異常食行動に関与している可能性が示唆された。

・脂質代謝異常（田中）

PWS の年長、成人例も VAT を少なく保ち、cardiovascular disease (CVD)のリスクを避けるためには、GH の長期投与が望ましいと考えられた。一方、VAT が多く adiponectin が低い PWS では、CVD に対し high risk であるため積極的な合併症治療介入が必要である。

・側彎症

PWS 症候群における成長ホルモン療法と側弯症の関連：急速進行例について

PWS 症候群患者においては、身長の伸び始める時期および歩行開始時期には側彎の発症に十分注意し、3 ヵ月毎に側彎症のチェックが必要である。

PWS における側彎症（58 例）と特発性側彎症（56 例）との比較研究（中村）

側彎変形は、PWS では腰椎・胸腰椎カーブが多く(Type 5, 6)、特発性では胸椎カーブが多かった(Type 1, 2, 3)。変形の各計測角度は、2 群間において違いはなかった。BMI は、PWS では大きい傾向が認められたが両群間で有意差はなかった。一方精神発達遅滞については PWS では 100%に認められた。

E. 結論

・精神神経症状

1) Prader-Willi 症候群と広汎性発達障害の心理行動症状の比較研究（井原、尾形）

Prader-Willi 症候群(PWS)を性別と遺伝子型に分類し、心理行動症状（WAIS - Ⅲ、PARS《広汎性発達障害評定尺度》、WHOQOL - 26）を比較検討した。性別においてはあまり性差が現われなかったが、遺伝子型においては UPD のほうが欠失よりも IQ が低く、広汎性発達障害特性が高い傾向があり、また母親の QOL も低かった。今後はサンプル数を増やし、PWS の心理行動症状の特性を明らかにし、問題行動への対応の指標を作成していきたい。

2) 日本人 Prader-Willi 症候群での痙攣の頻度と特徴（竹下）

日本の PWS 患者の痙攣合併の頻度は、海外の報告と同様で、人種間による差異はないと考えられた。半数以上が熱性痙攣であり、2 歳以降の発症は少ないため、

低年齢の PWS の発熱時には注意が必要だが、幼少期を過ぎると痙攣のリスクは減少すると考えられた。Angelman 症候群に認めるような特徴的な脳波所見は PWS にはなく、また難治に経過する例は少なかった。

3) Prader-Willi 症候群の脳血流の特性（小倉）

I123-iodoamphetamine を使用した triple-detector SPECT system により、PWS 患者の脳血流の評価を行った。その結果、島皮質の血流低下は、PWS の異常食行動に関与している可能性が示唆された。

・脂質代謝異常（田中）

GH 投与が脂質代謝に与える良好な影響が示唆された。

・側彎症

傍脊柱筋の増大率や左右差が側彎症の増悪因子であること、また、身長の伸び始める時期および歩行開始時期には側彎の発症に十分注意し、3 ヵ月毎に側彎症のチェックが必要であることが示唆された。

F. 健康危険情報

なし

G. 研究発表

1. 論文発表

1. Matsubara K, Murakami N, Nagai T, Ogata T. Maternal age effect on the development of Prader-Willi syndrome resulting from upd(15)mat through meiosis 1 errors. 2011, *J Hum Genet* 56(8):566-571
2. Tsuchiya T, Oto Y, Ayabe T, Obata K, Murakami N, Nagai T. Characterization of diabetes mellitus in Japanese Prader-Willi syndrome. 2011, *Clin Pediatr Endocrinol*, 20:33-38
3. Nakamura Y, Nagai T, Iida T, Ozeki S, Nohara Y. Growth hormone supplement treatment reduces the surgical risk for Prader-Willi syndrome patients. 2011, *Eur Spine J.* Published online
4. Oto Y, Obata K, Matsubara K, Kozu Y, Tsuchiya T, Sakazume S, Yoshino A, Murakami N, Ogata T, Nagai T. Growth Hormone Secretion and its Effect on Height in Pediatric Patients with Different Genotypes of Prader-Willi Syndrome. 2012, *Am J Med Genet A*, in Press.

2. 学会発表

1. European Human Genetics Conference 2011 (Amsterdam),
"Risk assessment of ART and its related factors in the development of Prader-Willi syndrome"
Keiko Matsubara, Nobuyuki Murakami, Satoru Sakazume, Yuji Oto, Toshiro Nagai, Tsutomu Ogata.
2. 第 34 回小児遺伝学会（横浜）
「ART および ART 関連因子は PWS の発症リスクとなるか？」
松原圭子、村上信行、坂爪悟、大戸祐二、緒方勤、永井敏郎
3. 61st, The American Society of Human Genetics (Montreal),
"Risk assessment of ART and its related factors in the development of Prader-Willi syndrome"
Keiko Matsubara, Nobuyuki Murakami, Satoru Sakazume, Yuji Oto, Toshiro Nagai, Tsutomu Ogata.
4. 第 45 回小児内分泌学会（大宮）
「ART および ART 関連因子は PWS の発症リスクとなるか？」
松原圭子、村上信行、佐藤智子、鏡雅代、永井敏郎、深見真紀、緒方勤
5. 第 56 回人類遺伝学会（千葉）
「ART および ART 関連因子は PWS の発症リスクとなるか？」
松原圭子、村上信行、佐藤智子、鏡雅代、永井敏郎、深見真紀、緒方勤
6. Prader-willi syndrome における側彎症手術例の検討　第 43 会日本側彎症学会 2009.11
7. 第２３回小児脂質研究会(福岡)「Prader-Willi 症候群（PWS)における成長ホルモン療法は高脂血症を改善する」田中百合子、土屋貴義、村上信行、永井敏郎
8. 第２５回小児脂質研究会(京都)「Prader Willi 症候群（PWS）の脂肪分布解析と成長ホルモン(GH)療法が分布に及ぼす影響について」阿部美子、田中百合子、村上信行、永井敏郎
9. 第２５回小児脂質研究会(京都)
「肥満 Prader-Willi 症候群(PWS)の脂肪分布の特徴-アディポサイトカインが高脂血症と糖尿病へ与える影響について-」
田中百合子、阿部美子、村上信行、永井敏郎
10. The growth hormone supplement reduces surgical risk for Prader-Willi patients IMAST Tronto July 21-21,2010
11. 7th International PWS Conference (Taipei)2010, "Growth hormon therapy improves hyperlipidemia in Prader-Willi Sydrome" Tanaka Y, Murakami N, Oto Y, Itabashi H, Tsuchiya T, Obata K, Nagai T

H. 知的財産権の出願・登録状況

1. 特許取得

なし

2. 実用新案登録

なし

研究成果の刊行一覧表

研究成果の刊行に関する一覧表

書籍

著者氏名	論文タイトル名	書籍全体の編集者名	書　籍　名	出版社名	出版地	出版年	ページ
永井敏郎	基本概念	永井敏郎	Prader-Willi症候群の基礎と臨床	診断と治療社	東京	2011	3-6
永井敏郎	成長パターン	永井敏郎	Prader-Willi症候群の基礎と臨床	診断と治療社	東京	2011	25-30
永井敏郎	生命予後と死因	永井敏郎	Prader-Willi症候群の基礎と臨床	診断と治療社	東京	2011	79-82
永井敏郎	成長ホルモン療法	永井敏郎	Prader-Willi症候群の基礎と臨床	診断と治療社	東京	2011	91-95
緒方勤 松原圭子	高齢出産に伴うPrader-Willi症候群病因の変化	永井敏郎	Prader-Willi症候群の基礎と臨床	診断と治療社	東京	2011	133-138
緒方勤 松原圭子	Prader-Willi症候群と生殖補助医療	永井敏郎	Prader-Willi症候群の基礎と臨床	診断と治療社	東京	2011	139-144
堀川玲子	耐糖能	永井敏郎	Prader-Willi症候群の基礎と臨床	診断と治療社	東京	2011	46-51
村上信行	筋力低下	永井敏郎	Prader-Willi症候群の基礎と臨床	診断と治療社	東京	2011	57-61
村上信行	側彎症	永井敏郎	Prader-Willi症候群の基礎と臨床	診断と治療社	東京	2011	62-68
中村豊	側彎症の外科的治療	永井敏郎	Prader-Willi症候群の基礎と臨床	診断と治療社	東京	2011	106-114

雑誌

発表者氏名	論文タイトル名	発表誌名	巻号	ページ	出版年
Matsubara K, Murakami N, Nagai T, Ogata T	Maternal age effect on the development of Prader-Willi syndrome resulting from upd(15)mat through meiosis 1 errors	J Hum Genet	56	566-571	2011
Tsuchiya T, Oto Y, Ayabe T, Obata K, Murakami N, Nagai T	Characterization of diabetes mellitus in Japanese Prader-Willi syndrome	Clin Pediatr Endocrinol	20	33-38	2011
Miyazaki O, Nishimura G, Kagami M, Ogata T	Radiological evaluation of dysmorphic thorax of paternal uniparental disomy 14.	Pediatr Radiol	41	1013-9	2011

Nakabayashi K, Trujillo AM, Tayama C, Camprubi C, Yoshida W, Lapunzina P, Sanchez A, Soejima H, Aburatani H, Nagae G, Ogata T, Hata K, Monk D	Methylation screening of reciprocal genome-wide UPDs identifies novel human-specific imprinted genes.	Hum Mol Genet	20	3188-97	2011
Yamazawa K, Nakabayashi K, Matsuoka K, Masubara K, Hata K, Horikawa R, Ogata T	Androgenetic/biparental mosaicism in a girl with Beckwith-Wiedemann syndrome-like and upd(14)pat-like phenotypes.	J Hum Genet.	56(1)	91-3	2011
Nakamura Y, Nagai T, Iida T, Ozeki S, Nohara Y	Growth hormone supplement treatment reduces the surgical risk for Prader-Willi syndrome patients	Eur Spine J		published online	2011
Sakazume S, Ohashi H, Sasaki Y, Harada N, Nakanishi K, Sato H, Emi M, Endoh K, Sohma R, Kido Y, Nagai T, Kubota T	Spread of X-chromosome inactivation into chromosome 15 is associated with Prader-Willi syndrome phenotype in a boy with a t(X;15)(p21.1;q11.2) translocation	Hum Genet	131	121-130	2012
Fuke-Sato T, Yamazawa K, Nakabayashi K, Matsubara K, Matsuoka K, Hasegawa T, Dobashi K, Ogata T.	Mosaic upd(7)mat in a patient with Silver-Russell syndrome	Am J Med Genet A	158A (2)	465-8	2012
Oto Y, Obata K, Matsubara K, Kozu Y, Tsuchiya T, Sakazume S, Yoshino A, Murakami N, Ogata T, Nagai T	Growth Hormone Secretion and its Effect on Height in Pediatric Patients with Different Genotypes of Prader-Willi Syndrome	Am J Med Genet A		in press	2012
Kagami M, Kato F, Matsubara K, Sato T, Nishimura G, Ogata T	Relative frequency of underlying genetic causes for the development of UPD(14)pat-like phenotype.	Eur J Hum Genet		in press	2012

研究成果の刊行物・別刷り

Journal of Human Genetics (2011) 56, 91–93

www.nature.com/jhg

SHORT COMMUNICATION

Androgenetic/biparental mosaicism in a girl with Beckwith–Wiedemann syndrome-like and upd(14)pat-like phenotypes

Kazuki Yamazawa[1,5], Kazuhiko Nakabayashi[2], Kentaro Matsuoka[3], Keiko Masubara[1], Kenichiro Hata[2], Reiko Horikawa[4] and Tsutomu Ogata[1]

This report describes androgenetic/biparental mosaicism in a 4-year-old Japanese girl with Beckwith–Wiedemann syndrome (BWS)-like and paternal uniparental disomy 14 (upd(14)pat)-like phenotypes. We performed methylation analysis for 18 differentially methylated regions on various chromosomes, genome-wide microsatellite analysis for a total of 90 loci and expression analysis of *SNRPN* in leukocytes. Consequently, she was found to have an androgenetic 46,XX cell lineage and a normal 46,XX cell lineage, with the frequency of the androgenetic cells being roughly calculated as 91% in leukocytes, 70% in tongue tissues and 79% in tonsil tissues. It is likely that, after a normal fertilization between an ovum and a sperm, the paternally derived pronucleus alone, but not the maternally derived pronucleus, underwent a mitotic division, resulting both in the generation of the androgenetic cell lineage by endoreplication of one blastomere containing a paternally derived pronucleus and in the formation of the normal cell lineage by union of paternally and maternally derived pronuclei. It appears that the extent of overall (epi)genetic aberrations exceeded the threshold level for the development of BWS-like and upd(14)pat-like phenotypes, but not for the occurrence of other imprinting disorders or recessive Mendelian disorders.
Journal of Human Genetics (2011) **56,** 91–93; doi:10.1038/jhg.2010.142; published online 11 November 2010

Keywords: androgenesis; Beckwith–Wiedemann syndrome; mosaicism; upd(14)pat

INTRODUCTION

A pure androgenetic human with paternal uniparental disomy for all chromosomes is incompatible with life because of genomic imprinting.[1,2] However, a human with an androgenetic cell lineage could be viable in the presence of a normal cell lineage. Indeed, an androgenetic cell lineage has been identified in six liveborn individuals with variable phenotypes.[3–7] All the androgenetic cell lineages have a 46,XX karyotype, and this is consistent with the lethality of an androgenetic 46,YY cell lineage.

Here, we report on a girl with androgenetic/biparental mosaicism, and discuss the underlying factors for the phenotypic development.

CASE REPORT

This patient was conceived naturally to non-consanguineous and healthy parents. At 24 weeks gestation, the mother was referred to us because of threatened premature delivery. Ultrasound studies showed Beckwith–Wiedemann syndrome (BWS)-like features,[8] such as macroglossia, organomegaly and umbilical hernia, together with polyhydramnios and placentomegaly. The mother repeatedly received amnioreduction and tocolysis.

She was delivered by an emergency cesarean section because of preterm rupture of membranes at 34 weeks of gestation. Her birth weight was 3730 g (+4.8 s.d. for gestational age), and her length 45.6 cm (+0.7 s.d.). The placenta weighed 1040 g (+7.3 s.d.).[9] She was admitted to a neonatal intensive care unit due to asphyxia. Physical examination confirmed a BWS-like phenotype. Notably, chest roentgenograms delineated mild bell-shaped thorax characteristic of paternal uniparental disomy 14 (upd(14)pat),[10] although coat hanger appearance of the ribs indicative of upd(14)pat was absent (Supplementary Figure 1). She was placed on mechanical ventilation for 2 months, and received tracheostomy, glossectomy and tonsillectomy in her infancy, due to upper airway obstruction. She also had several clinical features occasionally reported in BWS[8] (Supplementary Table 1). Her karyotype was 46,XX in all the 50 lymphocytes analyzed. On the last examination at 4 years of age, she showed postnatal growth failure and severe developmental retardation.

[1]Department of Molecular Endocrinology, National Research Institute for Child Health and Development, Tokyo, Japan; [2]Department of Maternal-Fetal Biology, National Research Institute for Child Health and Development, Tokyo, Japan; [3]Division of Pathology, National Medical Center for Children and Mothers, Tokyo, Japan and [4]Division of Endocrinology and Metabolism, National Medical Center for Children and Mothers, Tokyo, Japan
[5]Current address: Department of Physiology, Development & Neuroscience, University of Cambridge, Cambridge, UK.
Correspondence: Dr T Ogata, Department of Molecular Endocrinology, National Research Institute for Child Health and Development, 2-10-1 Ohkura, Setagaya, Tokyo 157-8535, Japan.
E-mail: tomogata@nch.go.jp
Received 9 September 2010; revised 18 October 2010; accepted 22 October 2010; published online 11 November 2010

MOLECULAR STUDIES

This study was approved by the Institutional Review Board Committee at the National Center for Child health and Development, and performed after obtaining informed consent.

Methylation analysis

We first performed bisulfite sequencing for the *H19*-DMR (differentially methylated region) and KvDMR1 as a screening of BWS[11,12] and that for the IG-DMR and the *MEG3*-DMR as a screening of upd(14)pat,[10] using leukocyte genomic DNA. Paternally derived clones were predominantly identified for the four DMRs examined (Figure 1a). We next performed combined bisulfite restriction analysis for multiple DMRs, as reported previously.[13] All the autosomal DMRs exhibited markedly skewed methylation patterns consistent with predominance of paternally inherited clones, whereas the *XIST*-DMR on the X chromosome showed a normal methylation pattern (Figure 1a).

Genome-wide microsatellite analysis

Microsatellite analysis was performed for 90 loci with high heterozygosities in the Japanese population.[14] Major peaks consistent with paternal uniparental isodisomy and minor peaks of maternal origin were identified for at least one locus on each chromosome, with the minor peaks of maternal origin being more obvious in tongue and tonsil tissues than in leukocytes (Figure 1b and Supplementary Table 2). There were no loci with three or four peaks indicative of chimerism. The frequency of the androgenetic cells was calculated as 91% in leukocytes, 70% in tongue cells and 79% in tonsil cells, although the estimation apparently was a rough one (for details, see Supplementary Methods).

Expression analysis

We examined *SNRPN* expression, because *SNRPN* showed strong expression in leukocytes (for details, see Supplementary Data). *SNRPN* expression was almost doubled in the leukocytes of this patient (Figure 1c).

DISCUSSION

These results suggest that this patient had an androgenetic 46,XX cell lineage and a normal 46,XX cell lineage. In this regard, both the androgenetic and the biparental cell lineages appear to have derived from a single sperm and a single ovum, because a single haploid genome of paternal origin and that of maternal origin were identified in this patient by genome-wide microsatellite analysis. Thus, it is likely that after a normal fertilization between an ovum and a sperm, the paternally derived pronucleus alone, but not the maternally derived pronucleus, underwent a mitotic division, resulting both in the generation of the androgenetic cell lineage by endoreplication of

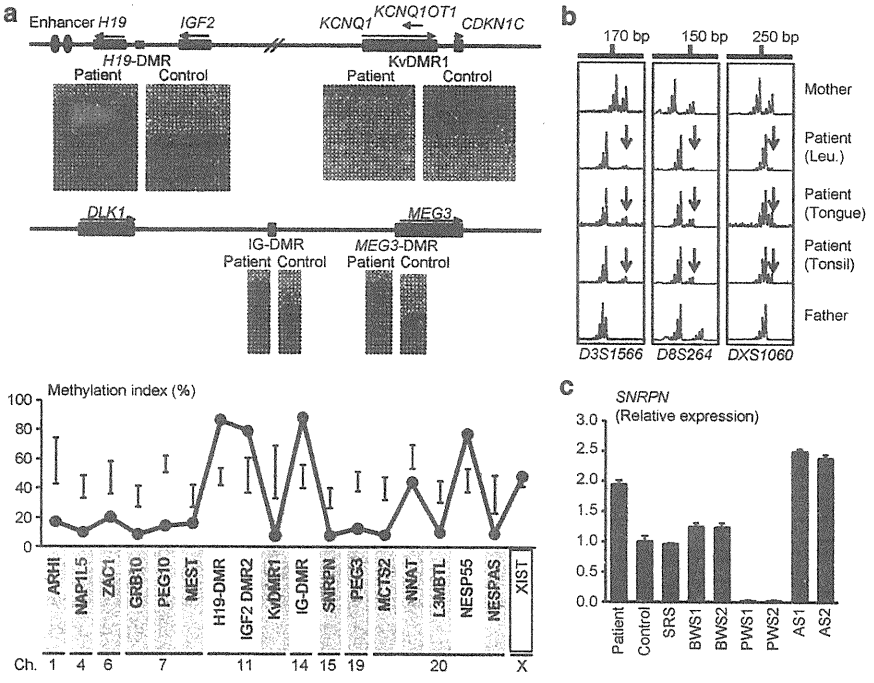

Figure 1 Representative molecular results. (**a**) Methylation analysis. Upper part: Bisulfite sequencing data for the *H19*-DMR and the KvDMR1 on 11p15.5, and those for the IG-DMR and the *MEG3*-DMR on 14q32.2. Each line indicates a single clone, and each circle denotes a CpG dinucleotide; filled and open circles represent methylated and unmethylated cytosines, respectively. Paternally expressed genes are shown in blue, maternally expressed gene in red, and the DMRs in green. The *H19*-DMR, the IG-DMR, and the *MEG3*-DMR are usually methylated after paternal transmission and unmethylated after maternal transmission, whereas the KvDMR1 is usually unmethylated after paternal transmission and methylated after maternal transmission.[10,11] Lower part: Methylation indices (the ratios of methylated clones) obtained from the COBRA analyses for the 18 DMRs. The DMRs highlighted in blue and pink are methylated after paternal and maternal transmissions, respectively. The black vertical bars indicate the reference data (maximum – minimum) in leukocyte genomic DNA of 20 normal control subjects (the *XIST*-DMR data are obtained from 16 control females). (**b**) Representative microsatellite analysis. Major peaks of paternal origin and minor peaks of maternal origin (red arrows) have been identified in this patient. The minor peaks of maternal origin are more obvious in tongue and tonsil tissues than in leukocytes (Leu.). (**c**) Relative expression level (mean ± s.d.) of *SNRPN*. The data are normalized against *TBP*. SRS: an SRS patient with an epimutation (hypomethylation) of the *H19*-DMR; BWS1: a BWS patient with an epimutation (hypermethylation) of the *H19*-DMR; BWS2: a BWS patient with upd(11)pat; PWS1: a Prader-Willi syndrome (PWS) patient with upd(15)mat; PWS2: a PWS patient with an epimutation (hypermethylation) of the *SNRPN*-DMR; AS1: an Angelman syndrome (AS) patient with upd(15)pat; and AS2: an AS patient with an epimutation (hypomethylation) of the *SNRPN*-DMR. The data were obtained using an ABI Prism 7000 Sequence Detection System (Applied Biosystems).

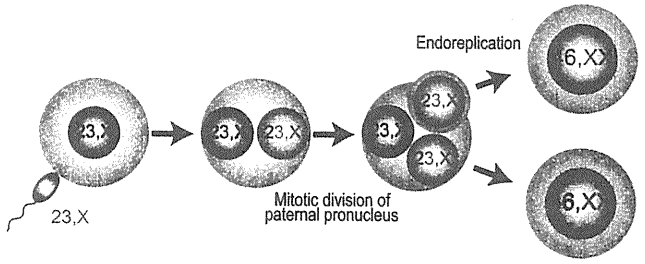

Figure 2 Schematic representation of the generation of the androgenetic/biparental mosaicism. Polar bodies are not shown.

one blastomere containing a paternally derived pronucleus and in the formation of the normal cell lineage by union of paternally and maternally derived pronuclei (Figure 2). This model has been proposed for androgenetic/biparental mosaicism generated after fertilization between a single ovum and a single sperm.[5,15,16] The normal methylation pattern of the *XIST*-DMR is explained by assuming that the two X chromosomes in the androgenetic cell lineage undergo random X-inactivation, as in the normal cell lineage. Furthermore, the results of microsatellite analysis imply that the androgenetic cells were more prevalent in leukocytes than in tongue and tonsil tissues.

A somatic androgenetic cell lineage has been identified in seven liveborn patients including this patient (Supplementary Table 1).[3–7] In this context, leukocytes are preferentially utilized for genetic analyses in human patients, and detailed examinations such as analyses of plural DMRs are necessary to detect an androgenetic cell lineage. Thus, the hitherto identified patients would be limited to those who had androgenetic cells as a predominant cell lineage in leukocytes probably because of a stochastic event and received detailed molecular studies. If so, an androgenetic cell lineage may not be so rare, and could be revealed by detailed analyses as well as examinations of additional tissues in patients with relatively complex phenotypes, as observed in the present patient.

Phenotypic features in androgenetic/biparental mosaicism would be determined by several factors. They include (1) the ratio of two cell lineages in various tissues/organs, (2) the number of imprinted domains relevant to specific features (for example, dysregulation of the imprinted domains on 11p15.5 and 14q32.2 is involved in placentomegaly[9,17]), (3) the degree of clinical effects of dysregulated imprinted domains (an (epi)dominant effect has been assumed for the 11p15.5 imprinted domains[18]), (4) expression levels of imprinted genes in androgenetic cells (although *SNRPN* expression of this patient was consistent with androgenetic cells being predominant in leukocytes, complicated expression patterns have been identified for several imprinted genes in both androgenetic and parthenogenetic fetal mice, probably because of perturbed *cis*- and *trans*-acting regulatory mechanisms[19]) and (5) unmasking of possible paternally inherited recessive mutation(s) in androgenetic cells. Thus, in this patient, it appears that the extent of overall (epi)genetic aberrations exceeded the threshold level for the development of BWS-like and upd(14)pat-like body and placental phenotypes, but remained below the threshold level for the occurrence of other imprinting disorders or recessive Mendelian disorders.

CONFLICT OF INTEREST

The authors declare no conflict of interest.

ACKNOWLEDGEMENTS

This work was supported by grants from the Ministry of Health, Labor, and Welfare, and the Ministry of Education, Science, Sports and Culture.

1 Surani, M. A., Barton, S. C. & Norris, M. L. Development of reconstituted mouse eggs suggests imprinting of the genome during gametogenesis. *Nature* **308,** 548–550 (1984).
2 McGrath, J. & Solter, D. Completion of mouse embryogenesis requires both the maternal and paternal genomes. *Cell* **37,** 179–183 (1984).
3 Hoban, P. R., Heighway, J., White, G. R., Baker, B., Gardner, J., Birch, J. M. *et al.* Genome-wide loss of maternal alleles in a nephrogenic rest and Wilms' tumour from a BWS patient. *Hum. Genet.* **95,** 651–656 (1995).
4 Bryke, C. R., Garber, A. T. & Israel, J. Evolution of a complex phenotype in a unique patient with a paternal uniparental disomy for every chromosome cell line and a normal biparental inheritance cell line. *Am. J. Hum. Genet.* **75**(Suppl), 831 (2004).
5 Giurgea, I., Sanlaville, D., Fournet, J. C., Sempoux, C., Bellanne-Chantelot, C. & Touati, G. Congenital hyperinsulinism and mosaic abnormalities of the ploidy. *J. Med. Genet.* **43,** 248–254 (2006).
6 Wilson, M., Peters, G., Bennetts, B., McGillivray, G., Wu, Z. H., Poon, C. *et al.* The clinical phenotype of mosaicism for genome-wide paternal uniparental disomy: two new reports. *Am. J. Med. Genet. Part A* **146A,** 137–148 (2008).
7 Reed, R. C., Beischel, L., Schoof, J., Johnson, J., Raff, M. L. & Kapur, R. P. Androgenetic/biparental mosaicism in an infant with hepatic mesenchymal hamartoma and placental mesenchymal dysplasia. *Pediatr. Dev. Pathol.* **11,** 377–383 (2008).
8 Jones, K. L. *Smith's Recognizable Patterns of Human Malformation* 6th edn. (Elsevier Saunders: Philadelphia, 2006).
9 Kagami, M., Yamazawa, K., Matsubara, K., Matsuo, N. & Ogata, T. Placentomegaly in paternal uniparental disomy for human chromosome 14. *Placenta* **29,** 760–761 (2008).
10 Kagami, M., Sekita, Y., Nishimura, G., Irie, M., Kato, F., Okada, M. *et al.* Deletions and epimutations affecting the human 14q32.2 imprinted region in individuals with paternal and maternal upd(14)-like phenotypes. *Nat. Genet.* **40,** 237–242 (2008).
11 Yamazawa, K., Kagami, M., Nagai, T., Kondoh, T., Onigata, K., Maeyama, K. *et al.* Molecular and clinical findings and their correlations in Silver-Russell syndrome: implications for a positive role of IGF2 in growth determination and differential imprinting regulation of the IGF2-H19 domain in bodies and placentas. *J. Mol. Med.* **86,** 1171–1181 (2008).
12 Weksberg, R., Shuman, C. & Beckwith, J. B. Beckwith-Wiedemann syndrome. *Eur. J. Hum. Genet.* **18,** 8–14 (2010).
13 Yamazawa, K., Nakabayashi, K., Kagami, M., Sato, T., Saitoh, S., Horikawa, R. *et al.* Parthenogenetic chimaerism/mosaicism with a Silver-Russell syndrome-like phenotype. *J. Med. Genet.* **47,** 782–785 (2010).
14 Ikari, K., Onda, H., Furushima, K., Maeda, S., Harata, S. & Takeda, J. Establishment of an optimized set of 406 microsatellite markers covering the whole genome for the Japanese population. *J. Hum. Genet.* **46,** 207–210 (2001).
15 Kaiser-Rogers, K. A., McFadden, D. E., Livesy, C. A., Dansereau, J., Jiang, R., Knops, J. F. *et al.* Androgenetic/biparental mosaicism causes placental mesenchymal dysplasia. *J. Med. Genet.* **43,** 187–192 (2006).
16 Kotzot, D. Complex and segmental uniparental disomy updated. *J. Med. Genet.* **45,** 545–556 (2008).
17 Monk, D., Arnaud, P., Apostolidou, S., Hills, F. A., Kelsey, G., Stanier, P. *et al.* Limited evolutionary conservation of imprinting in the human placenta. *Proc. Natl. Acad. Sci. USA.* **103,** 6623–6628 (2006).
18 Azzi, S., Rossignol, S., Steunou, V., Sas, T., Thibaud, N., Danton, F. *et al.* Multilocus methylation analysis in a large cohort of 11p15-related foetal growth disorders (Russell Silver and Beckwith Wiedemann syndromes) reveals simultaneous loss of methylation at paternal and maternal imprinted loci. *Hum. Mol. Genet.* **18,** 4724–4733 (2009).
19 Ogawa, H., Wu, Q., Komiyama, J., Obata, Y. & Kono, T. Disruption of parental-specific expression of imprinted genes in uniparental fetuses. *FEBS Lett.* **580,** 5377–5384 (2006).

Supplementary Information accompanies the paper on Journal of Human Genetics website (http://www.nature.com/jhg)

Journal of Human Genetics (2011) 56, 94–96

www.nature.com/jhg

SHORT COMMUNICATION

Low prevalence of classical galactosemia in Korean population

Beom Hee Lee[1,2,3,6], Chong Kun Cheon[4,6], Jae-Min Kim[2], Minji Kang[2], Joo Hyun Kim[2], Song Hyun Yang[5], Gu-Hwan Kim[2,3], Jin-ho Choi[1] and Han-Wook Yoo[1,2,3]

This study described the clinical and molecular genetic features of classical galactosemia in Korean population to contribute to the insight in the spectrum of galactosemia in the world, as little is known about the spectrum and incidence of galactosemia in Asia. During the 11-year study period, only three Korean children were identified as having classical galactosemia on the basis of the enzymatic and molecular genetic analysis. Asians have been reported to have mutations distinct from those of Caucasians and African Americans, indicating that galactose-1-phosphate uridyltransferase mutations are ethnically diverse. Our three patients had a total of three mutations (c.252+1G>A, p.Q169H and p.E363K), two of which were novel (p.E363K and c.252+1G>A) mutations. Interestingly, c.252+1G>A, which leads to skipping of exon 2, was observed in all three patients (three of six alleles), indicating that this mutation may be common in Koreans with classical galactosemia. Screening for classical galactosemia in 158 126 Korean newborns identified no patient with classical galactosemia. In conclusion, our findings provide further evidence for the ethnic diversity of classical galactosemia, which may be as rare in Koreans as in other Asian populations.

Journal of Human Genetics (2011) **56**, 94–96; doi:10.1038/jhg.2010.152; published online 9 December 2010

Keywords: ethnic divergence; galactosemia; GALT; mutation

Classical galactosemia (OMIM 230400) is caused by a deficiency in galactose-1-phosphate uridyltransferase (GALT; EC2.7.712). Classical galactosemia is characterized by more severe clinical manifestations than the other two types, galactosemia II or III, with newborns usually manifesting symptoms within a few days of birth after milk feeding.[1–3]

The incidence of classical galactosemia in western Europe has been estimated to be between 1:23 000 and 1:89 000.[1,4,5] In Korean newborns, the overall incidence of the three types of galactosemia have been reported to be approximately 1:40 000,[6] but the exact incidence of classical galactosemia is not yet known. Since the first report of a mutation in the *GALT* gene,[7] more than 200 different mutations have been identified with missense mutations being observed most commonly (http://www.hgmd.org).[1,8] The most common mutations in Caucasian and African American populations are p.Q188R and p.S135L, respectively,[9–11] but neither of these mutations have been detected to date in Asian populations. Similarly, Japanese patients have distinct mutations, such as p.V85_N97delinsRfsX8, p.W249X and p.R231H, which have not been observed in Caucasians and African Americans, providing further evidence for genetic heterogeneities among ethnic groups.[1,12,13]

Between March 1999 and May 2010, only three unrelated Korean patients were diagnosed with classical galactosemia at the Asan Medical Center, Seoul, Korea, with the diagnosis of each confirmed by enzyme assays and molecular genetic analysis (Table 1). All patients were identified by neonatal screening program performed at 3–5 days of life. Patients 1 and 2 had neonatal jaundice with slightly increased serum hepatic enzyme concentrations, which was not progressive, whereas patient 3 had clinically deteriorated and showed progressive jaundice and a bleeding tendency, while awaiting the results of screening tests that were reported on the eleventh day after birth (Table 1). Median total plasma galactose concentration was 50 mg per 100 ml (range, 13.5–68.9 mg per 100 ml; normal range <13 mg per 100 ml) and median erythrocyte galactose-1-phosphate concentration was 10.4 mg per 100 ml (range 1.60–62.8 mg per 100 ml; normal range <0.3 mg per 100 ml). The GALT activity was decreased in all patients, ranging from 0.1 to 0.8 umol hr^{-1} per gram hemoglobin (median, 0.3umol hr^{-1} per gram hemoglobin; normal range, 25.7 ± 3.6 umol hr^{-1} per gram hemoglobin) (Table 1). A galactose-restricted diet was effective in decreasing galactose and galactose-1-phosphate concentrations in all patients. The hepatic dysfunction, jaundice and

[1]Department of Pediatrics, Asan Medical Center Children's Hospital, University of Ulsan College of Medicine, Seoul, Korea; [2]Genome Research Center for Birth defects and Genetic Diseases, Asan Medical Center Children's Hospital, University of Ulsan College of Medicine, Seoul, Korea; [3]Medical Genetics Clinic and Laboratory, Asan Medical Center Children's Hospital, University of Ulsan College of Medicine, Seoul, Korea; [4]Department of Pediatrics, Genetic and Metabolic Clinic, Children Hospital, Pusan National University, Gyeongnam, South Korea and [5]Green Cross Reference Laboratory, Seoul, Korea
[6]These authors contributed equally to this paper as first authors.
Correspondence: Dr H-W Yoo, Genome Research Center for Birth defects and Genetic Diseases, Asan Medical Center Children's Hospital, University of Ulsan College of Medicine, 388-1 Pungnap-Dong, Songpa-Gu, Seoul 138-736, Korea.
E-mail: hwyoo@amc.seoul.kr
Received 13 September 2010; revised 14 October 2010; accepted 9 November 2010; published online 9 December 2010

Human Molecular Genetics, 2011, Vol. 20, No. 16 **3188–3197**
doi:10.1093/hmg/ddr224
Advance Access published on May 18, 2011

Methylation screening of reciprocal genome-wide UPDs identifies novel human-specific imprinted genes†

Kazuhiko Nakabayashi[1,‡,¶], Alex Martin Trujillo[3,¶], Chiharu Tayama[1], Cristina Camprubi[3], Wataru Yoshida[1], Pablo Lapunzina[4], Aurora Sanchez[5], Hidenobu Soejima[6], Hiroyuki Aburatani[7], Genta Nagae[7], Tsutomu Ogata[2], Kenichiro Hata[1] and David Monk[3,*,‡]

[1]Department of Maternal-Fetal Biology and [2]Department of Molecular Endocrinology, National Research Institute for Child Health and Development, Tokyo 157-8535, Japan, [3]Cancer Epigenetic and Biology Program (PEBC), Institut d'Investigació Biomedica de Bellvitge (IDIBELL), Hospital Duran i Reynals, Barcelona, Spain, [4]Instituto de Genética Médica y Molecular (INGEMM), CIBERER, IDIPAZ-Hospital Universitario La Paz, Universidad Autónoma de Madrid, Madrid, Spain, [5]Servei de Bioquímica i Genètica Molecular, CIBER de Enfermedades Raras, and Institut d'Investigacions Biomèdiques August Pi i Sunyer, Hospital Clínic, Barcelona, Spain, [6]Division of Molecular Genetics and Epigenetics, Department of Biomolecular Sciences, Faculty of Medicine, Saga University, Saga 849-8501, Japan and [7]Genome Science Division, Research Center for Advanced Science and Technology, the University of Tokyo, Tokyo 153-8904, Japan

Received April 11, 2011; Revised and Accepted May 13, 2011

Nuclear transfer experiments undertaken in the mid-80's revealed that both maternal and paternal genomes are necessary for normal development. This is due to genomic imprinting, an epigenetic mechanism that results in parent-of-origin monoallelic expression of genes regulated by germline-derived allelic methylation. To date, ~100 imprinted transcripts have been identified in mouse, with approximately two-thirds showing conservation in humans. It is currently unknown how many imprinted genes are present in humans, and to what extent these transcripts exhibit human-specific imprinted expression. This is mainly due to the fact that the majority of screens for imprinted genes have been undertaken in mouse, with subsequent analysis of the human orthologues. Utilizing extremely rare reciprocal genome-wide uniparental disomy samples presenting with Beckwith–Wiedemann and Silver–Russell syndrome-like phenotypes, we analyzed ~0.1% of CpG dinculeotides present in the human genome for imprinted differentially methylated regions (DMRs) using the Illumina Infinium methylation27 BeadChip microarray. This approach identified 15 imprinted DMRs associated with characterized imprinted domains, and confirmed the maternal methylation of the *RB1* DMR. In addition, we discovered two novel DMRs, first, one maternally methylated region overlapping the *FAM50B* promoter CpG island, which results in paternal expression of this retrotransposon. Secondly, we found a paternally methylated, bidirectional repressor located between maternally expressed *ZNF597* and *NAT15* genes. These three genes are biallelically expressed in mice due to lack of differential methylation, suggesting that these genes have become imprinted after the divergence of mouse and humans.

*To whom correspondence should be addressed. Tel: +34 932607500 ext. 7128; Fax: +34 2607219; Email: dmonk@idibell.cat
†Methylation array data: the data from the Illumna Infinium Human Methylation27 BeadChip microarray has been deposited with GEO database, accession number GSE28525.
‡Co-corresponding author. Tel: +81-3-3416-0181; Fax: +81-3-3417-2864; Email: knakabayashi@nch.go.jp
¶These authors contributed equally to this work.

INTRODUCTION

Genomic imprinting is an epigenetic process in which one allele is repressed, resulting in parent-of-origin specific monoallelic expression (1). To date, around 100 imprinted transcripts have been identified in mouse, including protein coding genes, long non-coding RNAs (ncRNA) and microRNAs. Approximately two-thirds show conserved imprinting status between mouse and humans, while some show imprinting restricted to humans (http://igc.otago.ac.nz/home.html).

Genomic imprinting is regulated by epigenetic modifications such as DNA methylation, along with repressive histone modifications that are transmitted through the gametes from the parental germlines (1). Many imprinted regions contain differentially methylated regions (DMRs) that exhibit parent-of-origin-dependent DNA methylation. Of the 21 known DMRs in mouse, a subset have been shown to function as *cis*-acting imprinting control regions (ICRs) orchestrating the monoallelic expression of genes over more than 100 kbp away (2). The establishment of imprinted methylation in both the maternal and paternal germlines requires the *de novo* DNA methyltransferae Dnmt3a and its related protein Dnmt3L (3,4). Maintenance of these DMRs is stable throughout somatic development and is regulated by Dnmt1 and Uhrf1 during DNA replication (5,6).

The identification of novel imprinted genes is important as it is becoming increasing evident that alterations in the fine-tuning of imprinted gene expression can influence a number of complex diseases such as obesity, diabetes, neurological diseases and cancer (7–9), in addition to the well-defined imprinting syndromes associated with severe disruption of imprinted domains.

The identification of imprinted genes has traditionally been performed in mouse owing to the ease of embryo and genetic manipulations, and has utilized gynogenetic and androgenetic embryos, or mice harboring regions of uniparental disomy (UPD), where two copies of an entire chromosome or chromosomal region is inherited from only one parent (reviewed in 10). These embryos have then been used in expression screen-based approaches such as subtractive hybridization, differential display or expression array hybridization (11,12). However, these screens are not deemed comprehensive, as imprinted gene expression can be both tissue- and developmental-stage specific. Previously, sophisticated screens have detected allelic differences in DNA methylation at imprinted DMRs present in all somatic tissues, irrespective of temporal and spatial expression. Techniques such as restriction landmark genomic screening, methylation-sensitive representation difference analysis (Me-RDA) and methylated DNA immunoprecipitation (MeDIP) have identified regions of allelic DNA methylation associated with chromosomal regions controlling several imprinted genes in mice (13–15) and humans (16,17).

In order to identify novel imprinted genes in humans, we have performed a quantitative genome-wide methylation screen comparing the methylomes of three-genome-wide paternal UPD (pUPD) samples identified with Beckwith–Wiedemann-like phenotypes and one genome-wide maternal UPD (mUPD) Silver–Russell-like syndrome case (18–21) with the methylomes of six normal somatic tissues. The genome-wide UPD samples were all mosaic, and we utilized DNA extracted from leukocytes as these presented with lowest level of the biparental cell line. The DNA methylation profiles of these samples only differ at imprinted DMRs, since they are all derived from leukocytes, making them ideal to screen for novel imprinted loci. We utilized the Illumina Infinium Human Methylation27 BeadChip microarray and were able to identify 15 imprinted DMRs associated with known imprinted transcripts, and confirm the allelic methylation within intron 2 of the *RB1* gene (22).

By comparing the methylation profiles of six somatic tissues and the genome-wide UPD cases, we identified a novel paternally methylated DMR which acts as a directional silencer resulting in the maternal expression of *ZNF597* (also known as *FLJ33071*) and *NAT15* on chromosome 16, and a maternally methylated DMRs encompassing the promoter region of the *FAM50B* retrotransposon on chromosome 6, which is paternally expressed in human tissues. Interestingly, the CpG islands of the mouse orthologues of *ZNF597*, *NAT15* and *FAM50B* are all unmethylated, resulting in biallelic expression in mid-gestation embryonic tissues.

RESULTS

Defining a hemimethylated data set

Almost all imprinted domains contain at least one region of allelic DNA methylation which is thought to regulate imprinting *in cis* (1). In order to identify new imprinted genes in humans, we performed a methyation screen of six different normal somatic tissues derived from the three germinal layers (placenta, leukocytes, brain, muscle, fat, buccal cells) and compared the data set with the methylation profiles from reciprocal genome-wide UPD samples. Genomic DNA was modified by sodium bisulfite treatment and hybridized to the Illumina Infinium Human Methylation27 platform. This array covers 27 578 CpG dinucleotides associated with 14 000 human genes. To identify novel imprinted DMRs, we took advantage of the fact that these CpG-rich sequences have a methylation profile of ~50% in all somatic tissues. We identified 78 CpG probes associated with 15 known imprinted DMRs on the array (average methylation 52%, SD 11.7) (Supplementary Material, Fig. S1). To define a range in which novel imprinted DMRs should lie, we used the mean for the known imprinted DMR ± 1.5 SD (range 34.4–69.6). After applying these defined cutoffs, we identified 3212 CpG probes for which the mean methylation value for all normal tissues was within this range. To rule out the possibility that a mean of ~52% was caused by extreme values of hyper- and hypomethylation as a result of tissue-specific methylation, we only assessed those within 1.8 times SD distance from the methylation average. This step ensures that the ~52% methylation value is representative of all tissues. Using these criteria, we reduced the data set to 1836 CpG probes, which were in addition to 72 probes mapping to known imprinted DMRs.

Determining the allelic methylation using genome-wide UPDs

To identify novel imprinted DMRs within the above hemimethylated data set outlined earlier, we compared the tissue methylation profiles to those obtained for the samples with genome-wide UPD. Of the 1836 CpG probes, only 14 gave methylation profiles consistent with an imprinted profile (Supplementary Material, Fig. S2). We subsequently mapped the exact location of the candidate CpGs using the genomic sequence of the unconverted DNA probes in the BLAT search tool (UCSC Genome Bioinformatics http://genome.ucsc.edu/). These 14 CpG probes were located close to nine autosomal genes, *RB1* (5), *FAM50B* (2), *ZNF597* (1), *TRPC3* (1), *SYCE1* (2), *TSP50* (1), *SORD* (1) and *ZBTB16* (1). We identified five independent probes located throughout CpG 85 (the CpG island identifier on the UCSC genome browser, build GRCh37/hg19) of the recently identified *RB1* imprinted gene on chromosome 13. These probes were unmethylated with average β-values of 0.21, 0.17 and 0.18 in the three genome-wide pUPD samples but hypermethylated, having an average β-value 0.88, in the genome-wide mUPD sample (a complete unmethylated CpG has a β-value of 0, and a fully methylated dinucleotide being 1). Using bisulphite PCR incorporating the single-nucleotide polymorphism (SNP) rs2804094 and sequencing of individual DNA strands, we were able to confirm that this 1.2 kb CpG island is a maternally methylated DMR in placenta, leukocyte and kidney-derived DNA and unmethylated in sperm (Supplementary Material, Fig. S3).

We identified one probe was located close to CpG 55 of the *TRPC3* gene on human chromosome 4 that was suggestive of a maternally methylated DMR. Subsequent allelic bisulphite PCR encompassing the SNP rs13121031 revealed that this region was subject to SNP-associated methylation and not parent-of-origin methylation (data not shown). The CpG islands within the promoters of *ZBTB16*, *TSP50* and *SORD* each had one probe that was suggestive of imprinted methylation, however allele-specific bisulphite PCR analysis revealed that these regions had a mosaic methylated profile (data not shown).

Two probes mapping to CpG 124 of *SYCE1/SPRNP1* on chromosome 10 also had a methylation profile consistent with an imprinted DMR. However, these probes were unable to discriminate *SYCE1* from *SPRN*, a second region that shared 93% homology. Due to the difficulty in designing bisulphite PCR primers that could specifically target *SYCE1*, we were unable to validate our initial observations.

The *ZNF597/NAT15* CpG island is a paternally methylated DMR

To date, only seven paternally methylated DMRs have been identified, the somatic DMRs at the *NESP*, *IGF2-P0* and *MEG3/GTL2* promoters, the germline *H19* differentially methylated domain (DMD), *Rasgrf1* DMD, IG-DMR and *ZDBF2* DMR (15,23–26). The *RASGRF1* is not imprinted in humans due to lack of the DNA repeat elements that are involved in establishing germline methylation (27). We identify two CpG probes, one mapping to CpG 41 between the promoters of *ZNF597* and *NAT15*, the other 500 bp away, in a region flanking CpG 41. Both probes were hypermethylated in the three genome-wide pUPD samples (β-values of 0.83, 0.42, 0.75) and hypomethylated (β-value of 0.08) in the genome-wide mUPD sample. Using bisulphite PCR and subsequent sequencing of heterozygous DNA samples for the SNP rs2270499, we were able to confirm that the methylation was solely on the paternally derived allele in placenta, leukocyte and kidney (Fig. 1). This is consistent with the previous report that *ZNF597* is maternally expressed in human leukocytes (28). Bisulphite PCR and sequencing of sperm DNA revealed that this region lack methylation, indicating that CpG41 is not a germline DMR. Using allele-specific RT–PCR that incorporated coding SNPs within exon 3, we observed maternal expression in brain ($n = 1$) and placenta ($n = 3$), and confirmed imprinting in leukocytes ($n = 2$).

The gene encoding *N*-acetyltransferase 15, *NAT15*, is encoded by two different transcripts (Fig. 1A). To determine whether *NAT15* is also subject to genomic imprinting, we performed allelic RT–PCR using PCR primers that could discriminate each isoform. We find that *NAT15* isoform 1 is maternally expressed in both placenta ($n = 5$) and leukocytes ($n = 1$), whereas isoform 2 is biallelically expressed ($n = 4$) which is consistent with CpG 101 being unmethylated (Fig. 1, data not shown).

FAM50B DMR shows graduated methylation

We identified two probes mapping to a 1.7 kbp CpG island within the *FAM50B* promoter. These probes were hypermethylated in the genome-wide mUPD (average β-values of 0.86), but hypomethylation in the three pUPD samples mUPD (β-value of 0.23, 0.39, 0.31). Allelic bisulphite sequencing showed that the methylation profile of CpG 143 differs between the 5′ and 3′ ends. The 5′ region flanking the SNP rs2239713, overlapping the *FAM50B* promoter, is a maternally methylated DMR in placenta-, leukocyte- and kidney-derived DNA, while the 3′ region near rs34635612 is fully methylated on both parental alleles. Despite this methylation gradient, the *FAM50B* gene is paternally expressed in placenta ($n = 6$) (Fig. 2).

The absence of allelic methylation at the mouse orthologues *of ZNF597, NAT15* and *FAM50B* is associated with biallelic expression

To determine whether the allelic expression of the novel imprinted transcripts was conserved in mouse, we investigated the allele-specific expression using RT–PCR amplification across transcribed SNPs. Mouse tissues were derived from interspecies crosses at both embryonic day E9.5 and post-natal day 1. The *Fam50b* gene has two isoforms with alternative first exons. We could only detect expression in testis, which was derived from both parental alleles. Exon 2 of Fam50b corresponds to an X-chromosome-derived retrogene and overlaps a methylated CpG island.

The *Nat15* and *Znf597* genes share two different promoter CpG islands, CpG 35 and CpG 87 that are orthologous to the *ZNF597* DMR and the *NAT15* isoform 2 promoters, respectively. In mouse, both of these regions are unmethylated. Both *Nat15* isoforms are predominantly expressed in

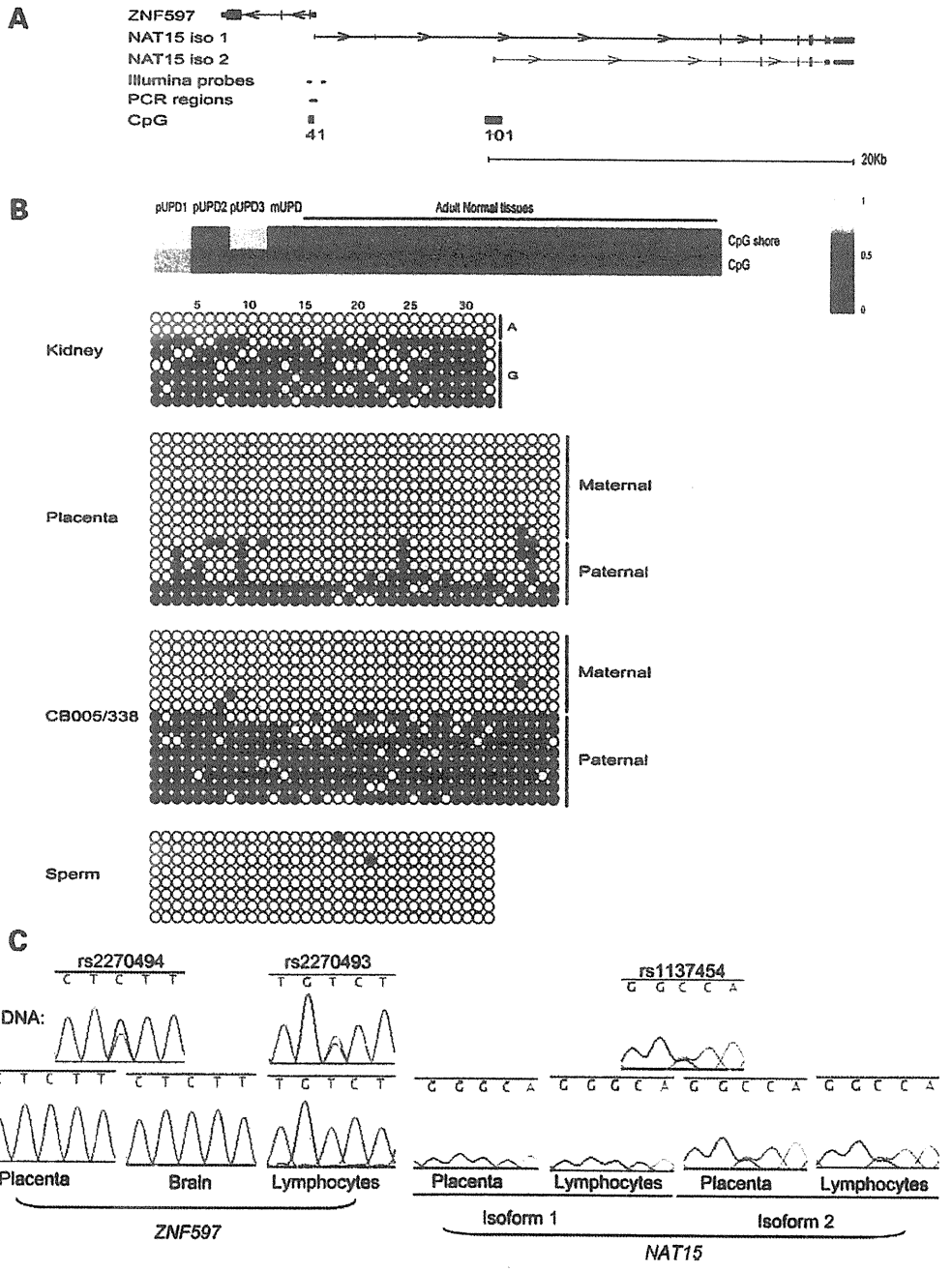

Figure 1. (A) Map of the *ZNF597-NAT15* locus on human chromosome 16, showing the location of the various transcripts, CpG islands, Illumina probes and bisulphite PCR regions (red transcripts are maternally expressed, blue paternally expressed and grey are expressed from both parental alleles. Arrows represent the direction of transcription) (not drawn to scale). (B) Heat map of the Infinium HumanMethylation27 BeadChIP for the *ZNF597* CpG probes (cg24333473 in CpG island; cg14654875 in CpG shore), with confirmation of allelic methylation in kidney, placenta and cord blood derived DNA. Each circle represents a single CpG dinucleotide and the strand, a methylated cytosine (filled circle) or an unmethylated cytosine (open circle). The same region was analyzed in sperm-derived DNA. (C) The sequence traces show allelic expression for the *ZNF597* and *NAT15* genes.

brain and testis, which is equally derived from both parental alleles. The variants of *Znf597* were expressed in E9.5 whole embryo, yolk sac and placenta, and in individual tissues later in development. Allelic expression analysis revealed that these transcripts were not imprinted, with equal expression from both parental chromosomes (Fig. 3).

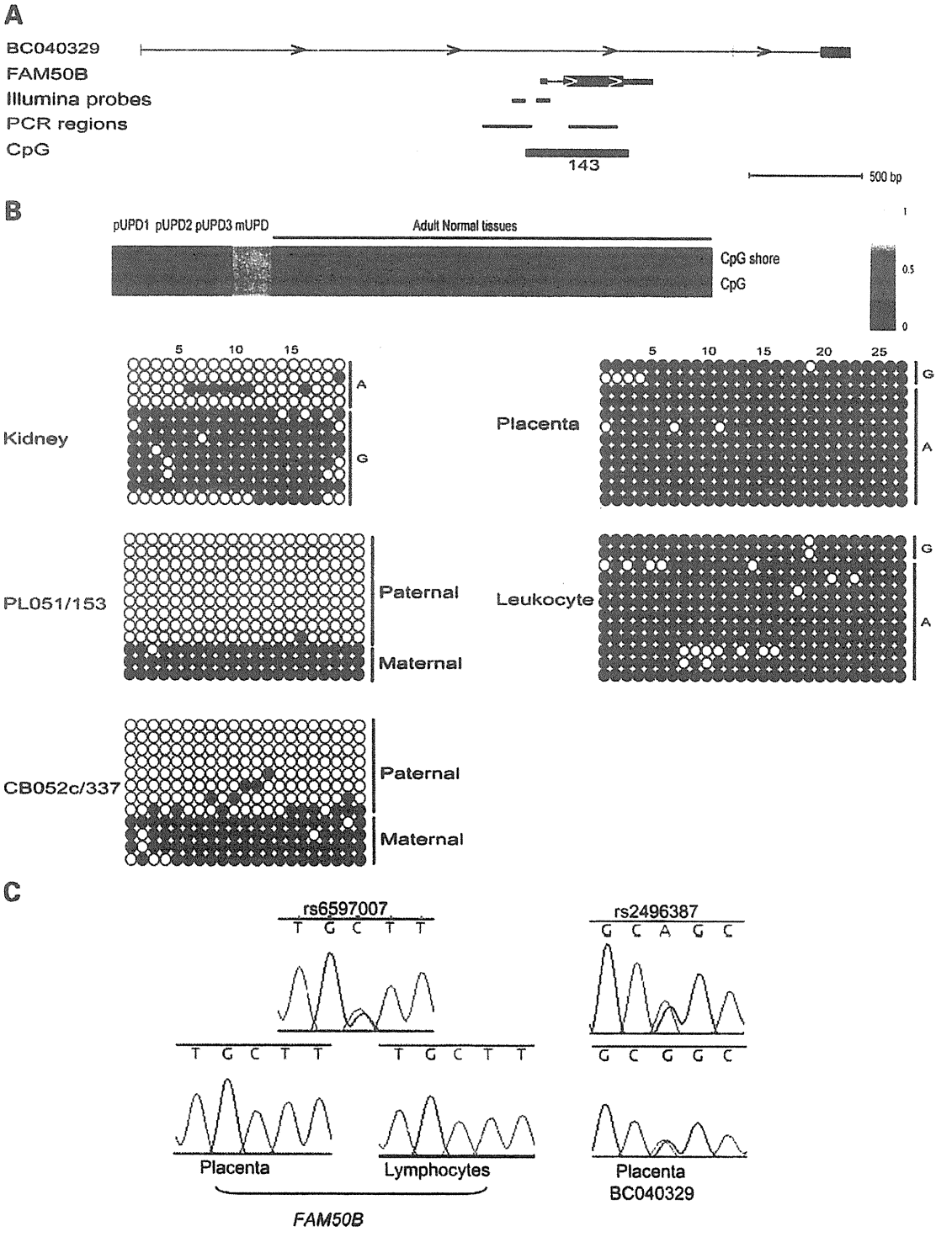

Figure 2. (A) A map of the *FAM50B/BC040329* locus, with the location of the of the CpG island (not to scale). (B) Heat map for CpG probes mapping to the *FAM50B* promoter (cg01570885; cg03202897) and the subsequent analysis of allelic methylation in various tissues. The methylation profiles on the left are from the 5′ CpG island region, while those on the right are from the 3′ region. (C) The allelic expression of *FAM50B* and the host gene in term placenta and leukocytes.

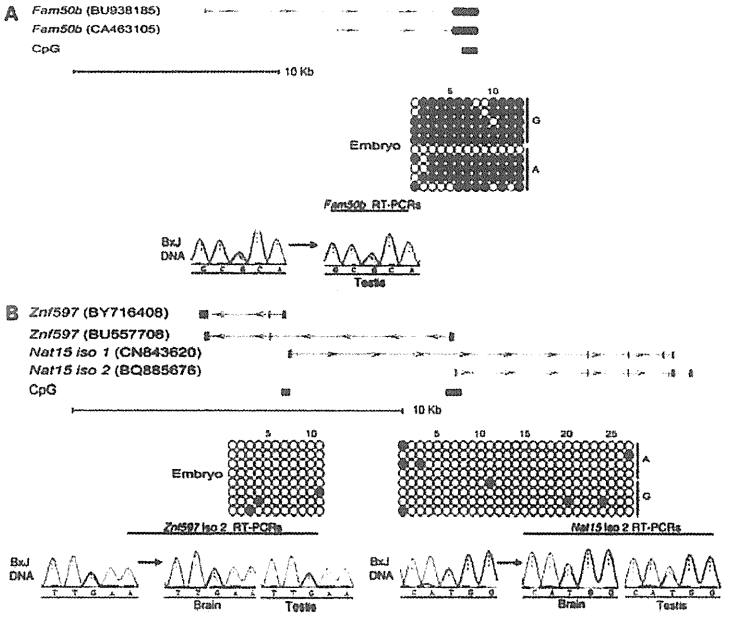

Figure 3. Schematic maps of the *Fam50b* (A) and *Znf597/Nat15* genes (B), with the location of the alternative promoter regions. The methylation status of the orthologous CpG islands associated with each domain was examined in embryo-derived DNA. The allelic expression of each gene in various mouse tissues from reciprocal mouse crosses. For clarity, only the expression in B6 × JF1 tissues is shown.

DISCUSSION

Identification of new human imprinted genes requires screening human samples

Most screens for new imprinted genes are undertaken in mouse with subsequent confirmation of the imprinting status of the human orthologues. Despite the success, this approach will not identify imprinted loci specifically imprinted in humans. To date, very few imprinted genes are human-specific, however, these rare transcripts do exist as highlighted by the paternally expressed *L3MBTL, C19MC* and *RB1* genes (22,29,30). Using DNA from Beckwith–Wiedemann and Silver–Russell-like phenotypes with reciprocal genome-wide UPDs, we have performed a comprehensive screen of ~0.1% of the human methylome. Despite the extensive coverage of Illumina Infinium Human Methylation27 BeadChip microarray, we identified very few novel imprinted loci. However, it must be noted that paternal germline DMRs are not associated with CpG islands, and therefore maybe remote from gene promoters and promoter CpG islands present on the array.

The predicted number of imprinted genes varies with estimates from 200–2000 transcripts in mouse, with one transcriptome-wide analysis, using the ultra sensitive RNA-seq technology, identifying over 1000 transcripts in brain with parent-of-origin expression bias (31). Recent studies have predicted and experimentally verified imprinted genes based on sequence and epigenetic characteristics. For example, human imprinted regions significantly lack short interspersed transposable elements in comparison with the rest of the genome and are associated with CpG islands (32,33). Using a bioinformatics approach, Luedi *et al.* (34) predicted 156 imprinted genes in humans based on similarity with known imprinted transcripts, confirming the maternal expression of *KCNK9*. In addition, the paternally expressed *MCTS2* gene was identified through a hypothesis-driven search for intronic X-chromosome-derived retrotransposons that are associated with CpG island promoters (35). Interestingly, *FAM50B* is also an imprinted X-chromosome-derived retrogene and was correctly identified by Luedi *et al.* (34) during their computational screening and the imprinting status recently confirmed (36).

We wished to identify additional imprinted loci based on data generated in previously published analyses. We have compared our hemimethylated data set against the 156 bio-informatically predicted imprinted genes and the 82 candidates predicted due to unequal representation of alleles in public EST libraries and expression genotype arrays (37,38). We found that fifteen out of one hundred and fifty-six and nine out of eighty-two, respectively, were present in our data set. However, none of these additional genes had a methylation profile consistent with an imprinted DMR, highlighting the high false-positive rates of bioinformatic predictions (Supplementary Material, Fig. S4). From our observations, we predict that the majority of human DMRs overlapping promoters have been identified. Following analysis of more than 14 000 genes, we identified only two new imprinted DMRs. Extrapolating this trend to the 34 702 annotated RefSeq genes, we predict that there will be around five additional unidentified DMRs in the human genome, resulting in a total of ~35.

Parent-of-origin DNA methylation is not the only epigenetic signature associated with imprinted DMRs (reviewed in 9). Recently, a chromatin signature has been shown to mark imprinted DMRs; with trimethylation of lysine 9 of histone

H3 (H3K9me3) and trimethylation of lysine 20 of histone H4 (H4K20me3) associated with the DNA methylated allele (39), while the unmethylated allele is enriched for the transcriptionally permissive Lysine 4 methylation of histone H3 (H3K4me2/3) (40). The combination of differential DNA methylation between sperm and somatic tissues and an overlapping H3K9me3 and H3K4me3 signature has recently been used to identify 11 new candidate DMRs in mouse (41). With the availability of human ChIP-seq derived genome-wide data sets for most histone modifications (42,43), it would be interesting to determine if this histone signature recognized in mouse can be used to identify novel human imprinted DMRs. Interrogation of the NHLBI ChIP-seq data set (http://dir.nhlbi.nih.gov/papers/lmi/epigenomes/hgtcell.aspx) revealed that the *RB1*, *ZNF597* and *FAM50B* DMRs are enriched for both H3K4me3 and H3K9me3, with the later two regions harboring functional CTCF binding sites (data not shown).

The regulation of imprinted domains on human chromosomes 13 and 16

The *RB1* DMR has previously been proposed to contain the promoter of the paternally expressed *E2B-RB1* isoform (22). We were unable to identify coding SNPs within the *RB1* gene that would allow us to determine the allelic expression in our cohort of tissues. However, we were able to show that the *LPAR6* gene, encoding lysophosphatidic acid receptor 6 located in intron 16 of *RB1* is biallelically expressed, suggesting that the *RB1* DMR does not influence the expression of this gene (Supplementary Material, Fig. S3).

The maternal expression of *ZNF597* has previously been shown in leukocytes (28). Here, we show that the *ZNF597* DMR acts as a bidirectional silencer, which orchestrates the paternal silencing of *ZNF597* and *NAT15*. This organization is reminiscent of *PEG10-SGCE* domain on human 7p22 (44). We did not observe methylation in DNA isolated from mature sperm, which suggests that this region acquires methylation during early somatic development (Fig. 1). All known somatic DMR are associated with nearby germline DMRs, which regulate the methylation in a hierarchical fashion (23,45,46), implying a yet to be identified germline DMR is situated within the vicinity of the *ZNF597* gene.

The maternally expressed *NAT15* is a highly conserved protein coding gene with two alternative first exons, with only isoform I subject to imprinting. In addition, there is evidence from EST libraries of an ncRNA (genbank: DA387972) that originates from the *NAT15* isoform 1 promoter and continues past the exon–intron splice site to produce a ~550 bp transcript. Unfortunately, we were unable to detect expression of this transcript in our tissue set, so we could not determine if this ncRNA is imprinted.

FAM50B is an imprinted retrogene

Sequence analysis revealed that the *FAM50B* transcript (previously named *X5L*) is a retrotransposon that originated from *FAM50A/XAP5* within Xq28. Unlike other classical retrogenes, this gene has an intron in the 5′ UTR in both humans and mouse, which has no counterpart in its parental gene. It is likely that the intron was inserted after retroposition, possibly during recruitment of a functional promoter region (47). Interestingly, several other imprinted genes have been shown to originate from retrotransposition from the X-chromosome genes (35,48). *FAM50B* is ubiquitously expressed, and is inserted within the intron of a host transcript *BC040329*, which is predominantly expressed in testis with low detection in brain and placenta (data not shown). This host gene is biallelically expressed in placenta ($n = 7$) (Fig. 2), of which two samples exhibited imprinted expression of *FAM50B*.

Discrepancy between imprinted DMR methylation screens

The quantitative methylation values obtained using the Illumina Infinium platform makes it suitable for comparing reference and test samples. This approach has previously been used to screen for imprinted DMRs using paternally derived androgenetic complete hydatidiform moles versus maternally derived mature cystic ovarian teratomas and in patients with maternal hypomethylation syndrome (24,49). In both cases, the genetic material analyzed is not ideally suited for comprehensive screening for novel imprinted loci. This is because it is currently unknown to what extent the DNA methylation profile is altered in ovarian teratomas, and any differences maybe due to the uniparental nature of the sample or tumorgenic changes, and candidates obtained from comparisons with complete hydatidiform moles may simply reflect tissue-specific differences. This is highlighted by the fact that of the 95 candidate probes identified by Choufani *et al.* (49), 68 overlapped with our hemimethylated data set (Supplementary Material, Fig. S4) with only *ZNF597* DMR being identified in both screens. These authors also suggest that *AXL*-promoter region is a DMR, but this was not identified using our genome-wide UPDs, and bisulphite PCR and sequencing of our samples revealed a non-allelic mosaic methylation profile (Supplementary Material, Fig. S5). In addition, the methylation profiles obtained from comparing normal and maternal hypomethylation samples will only facilitate the identification of a subset of imprinted DMRs, since *ZFP57* mutations do not effect the maintenance of all maternally methylated imprinted DMRs equally (50,51).

Functional relevance of the new imprinted domains

Very little is known about the role of *FAM50B*, *ZNF597* and *NAT15*, with no previous publications describing functional studies. The three new imprinted regions we identify all map to chromosomes for which recurrent chromosomal UPDs have been reported. With the exception of pUPD and the overexpression of *PLAGL1/HYMAI* in Transient Neonatal Diabetes Mellitus, the UPDs for these chromosomes are not associated with obvious developmental phenotypes and most cases were identified because of the unmasking of mutant recessive alleles (reviewed in 52,53).

CONCLUSIONS

Our study has assisted in defining a comprehensive catalog of human imprinted genes. The use of extremely rare reciprocal